KGS Fall '98 National Conference / November 6~7, 1998 /Seoul / Korea

Application of Soil Nailing under Piled Bridge Abutment
강관 파일로 지지된 교대하부에서의 쏘일 네일링 적용

임 유 진[1], Lim, Yu-Jin

[1] 한국도로공사 도로연구소 지반연구실 책임연구원
Chief Researcher, Highway Research Center, Korea Highway Corporation

개요(Synopsis)

강관파일로 지지되고 있는 교대하부의 기존 도로를 확장하기 위하여 교대전면의 압성토를 순차적으로 제거할 때의 교대 및 굴착면의 안정성을 확보하기위한 보강방법으로 쏘일 네일링을 선택하였다. 기존 구조체와 쏘일네일벽체 사이의 상호작용은 매우 복잡하여, 이때 문제가 될 수 있는 것은 기존 파일에 추가로 작용하는 축압축력과 휨모멘트의 크기, 네일의 인장력 크기, 그리고 벽체의 변위를 들 수 있다. 이와같은 복잡한 거동을 분석하기 위하여 모든 구조물을 포함하면서 네일타설 등의 全 축조순서를 고려할 수 있는 3차원 유한요소해석 기법을 제안하였다. 제안된 해석기법의 타당성을 검증하기 위하여 현장 실계측 값과 비교, 평가하였다. 아울러 여러 가지 매개변수를 변화시키며 수치해석을 실시하였으며, 이 결과 기존의 설계법으로서는 확인할 수 없었던 각 구조체 사이에 작용하는 힘 등에 대한 유용한 정보를 구할 수 있었다.

Key words: Piled bridge abutment, soil nailing, finite element analysis, hyperbolic model

1.Introduction

The soil nailed wall technology is approximately 25years old and many investigators have contributed to the proper design of such retaining structures. Among these are Stocker et al. (1979), Sclosser (1983), Juran et al. (1990), and CALTRANS (1994). Soil nailed walls under piled bridge abutments represents a new application of soil nailing (Fig. 1.). The impact of removing the sloped embankment in front of the abutment has not been studied in detail, however. Do the piles carry more load and more bending moment? What load exists in the nails? What deflection magnitude can one expect for such soil nailed walls? Some of the questions prompted this study (Lim and Briaud, 1996). Because the problem is a true three-dimensional problem, the selected methodology is a three-dimensional numerical simulation. The Finite Element Method (FEM) is used to simulate the abutment, the piles, the slope, the soil, and the nails together with a proper excavation sequence. Details on the set up of the FEM is presented by Briaud and Lim (1997). The results of this numerical study are used to suggest some design guidelines.

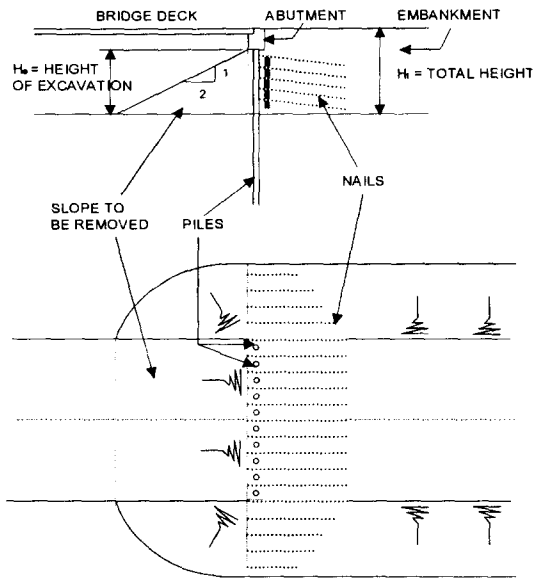

Fig. 1 Soil Nailed Wall under Piled Bridge Abutment

2. SIMULATED WALL SECTION

A repetitive section of the wall was chosen for the simulation. It was found that the best section was one that would include one vertical pile, an adjacent stack of inclined nails and the soil mass with boundaries located halfway between a pile and a stack of nails. The width of the mesh for the case history was 1.37m which corresponds to the spacing between piles and the spacing between the nails. Special moment restrains were required on the vertical edge boundaries of the wall in order to maintain a right angle in plan view between the displaced wall face and sides of the simulated wall section.

3. MODELING OF SOIL AND STRUCTURAL ELEMENTS

The general purpose Finite Element code ABAQUS (Hibbit, Karlson and Sorensen, 1992) was used for all the runs. The piles and the nails were simulated with one-dimensional beam elements. In choosing the axial and bending stiffnesses of the nail elements both the grout annulus and the steel tendon were included.

The shotcrete facing was simulated with two dimensional shell elements. The abutment and pile cap were simulated with 8-node brick elements. All the structural elements were modeled by linear elasticity.

The soil was simulated with 8 noded brick elements. The soil model was a modified Duncan-Chang hyperbolic model (Seed and Duncan, 1984). This model is a nonlinear model which includes the influence of the stress level on the stiffness, on the strength, and on the volume change characteristics of the soil. With this model it was also possible to simulate the hysteresis of the soil by unloading and reloading the soil along a path different from the primary loading path.

The expression that gives tangent Young's modulus, E_t for the hyperbolic model is:

$$E_t = \left(1 - \frac{R_f(1-\sin\phi)(\sigma_1 - \sigma_3)}{2(c\cos\phi + \sigma_3 \sin\phi)}\right)^2 K P_a \left(\frac{\sigma_3}{P_a}\right)^n \qquad (1)$$

where σ1 and 3 are the major and minor effective principal stresses in a soil element. Pa is the atmospheric pressure.

The unload-reload modulus, Eur is given by:

$$E_{ur} = K_{ur} P_a \left(\frac{\sigma_3}{P_a}\right)^n \tag{2}$$

The characteristics of volume change of a soil can be described by Poissons ratio when Hookes law is adapted as a constitutive model. The tangent Poissons ratio ν_t is defined as:

$$\nu_t = 0.5 - \frac{E_t}{6 B_t} \tag{3}$$

where the tangent bulk modulus Bt is given by:

$$B_t = K_B P_a \left(\frac{\sigma_3}{P_a}\right)^{n_B} \tag{4}$$

Seed and Duncan (1984) have suggested minor modifications with respect to the limiting values of B_t and the criterion for unloading-reloading. In the original model (Duncan and Chang, 1970), to verify whether a soil element is being loaded or unloaded, the stress level(SL) criterion is used. However, it has been acknowledged that the simple stress-level criteria for assignment of unloading-reloading moduli should be modified to include consideration of variations in the confining pressure as well. The criterion based on the stress state(SS) concept to separate loading from unloading was used in this study.

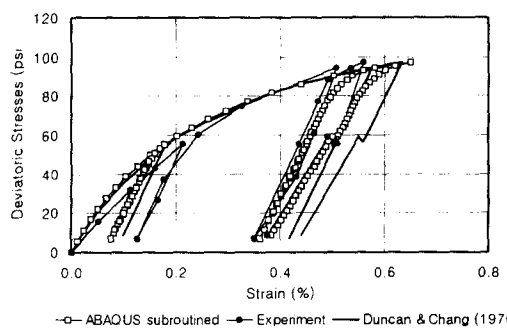

Fig. 2. Stress-Strain Curves for Loose Silica Sand under Complex Loading Conditions

This hyperbolic model was coded in FORTRAN and implemented into ABAQUS as a user defined subroutine UMAT. To verify the subroutine with respect to the logical consequence of the algorithm as well as the proper linking with the main program, the result of the finite element analysis performed by ABAQUS with the material subroutine UMAT were compared with the results by Duncan and Chang (1970) as shown in Fig. 2. The overall agreement is quite good.

4. SIMULATING THE EXCAVATION SEQUENCE

The full construction sequence adapted in this study can be summarized as shown in Fig. 3. The initial shape of the mesh was a rectangular box 166.2m long, 25m high, and 1.37m wide.

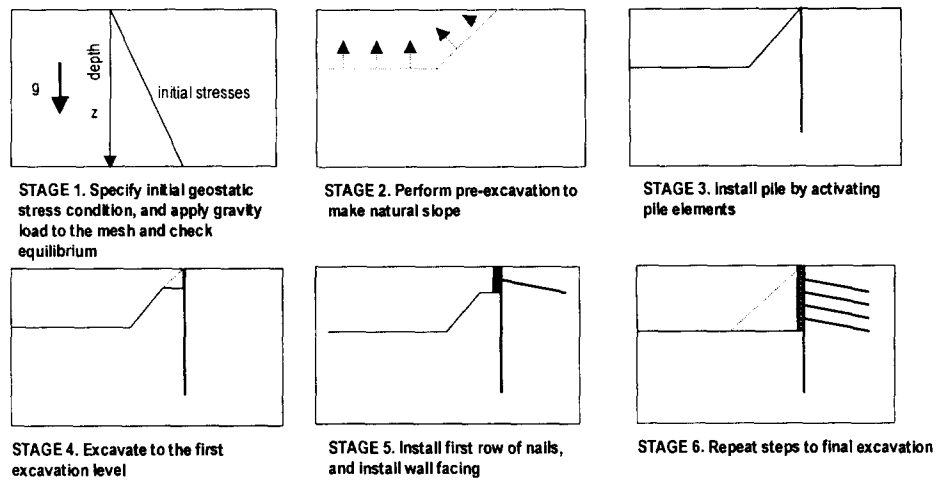

Fig. 3. Simulation of Construction Sequence

5. I-5 Swift-Delta Soil Nailed Wall

To widen the road below the Oregon Slough Bridge near Portland, the existing slope in front of the South abutment was excavated and a soil-nailed wall was constructed. The abutment was on concrete-filled steel pipe piles that were 0.36m diameter, with a 6.35 mm wall thickness and with the pile tip 22.9m below the bridge deck.

The soil information including SPT blow counts is shown in Fig. 4. The construction of this 50m long and 5.3m high wall consisted of six excavation lifts with the placement of five rows of nails.

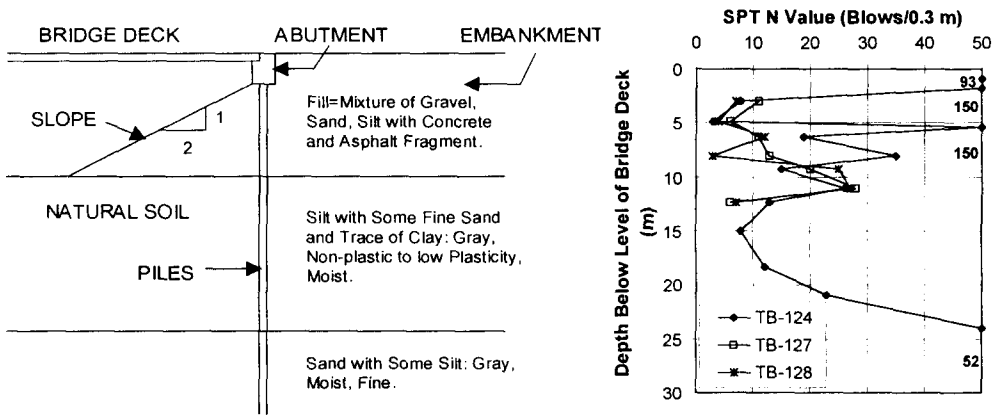

Fig. 4. Soil Stratigraphy for I-5 Swift-Delta Bridge

6. Calibration of Model against I-5 Soil Nailed Wall and Results

The soil parameters were obtained from the calibration process to match the measured axial force with the calculated one versus length distributions for all the instrumented nails after the last step of excavation. The most influential input parameter was K_o,

followed by K and then by the bending stiffness of the shotcrete facing. The final comparison between measured and predicted axial nail force distribution is shown in Fig. 5. The comparison between predicted wall deflections and various measurements is shown in Fig. 6. It was found that the wall deflection profile with depth under the abutment disclosed cantilever movement. However, the wall deflection profile with depth outside bridge represented deep inward movement even though the ground is sandy soil.

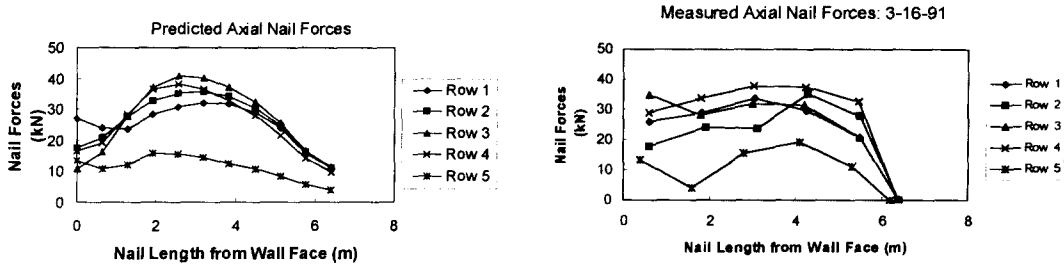

Fig. 5. Comparison of Measured and Predicted Axial Nail Forces after Final Excavation

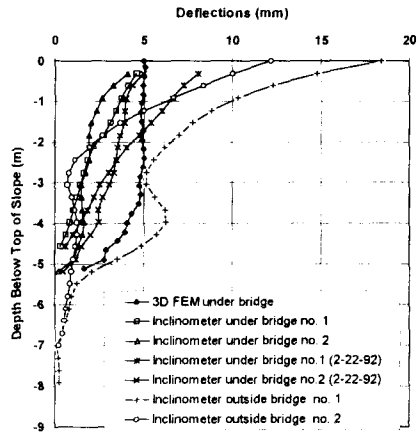

Fig.6. Comparison of Wall Deflection

7. Results from Numerical Simulation

It is assumed here that matching the axial nail force versus length distributions for all instrumented nails leads to reasonably close predictions of all other aspects of the wall behavior.

7.1 Apparent Earth Pressure and Tensile Force in Nails

For each nail, an apparent earth pressure p was obtained by calculating the ratio of the maximum nail force T_{max} over the tributary area of wall facing for that nail

The abutment and pile cap were not considered as part of the tributary area for the top nail. The results show (Fig.7.) that the maximum value of p is close to $0.65K_a\gamma H_t$ where K_a is the active earth pressure coefficient, γ the soil effective unit weight, and H_t the total height from the level of the bridge deck to the bottom of the slope. The $0.65K_a\gamma H_t$ value or the distribution of p is similar to the one proposed by Terzaghi and Peck (1967) for braced excavation except for the decrease of p in the bottom $0.25H_e$. Indeed the bottom nail carries much less load that the others. The $0.65K_a\gamma H_t$ value for p is similar to the one proposed by Juran and Elias(1987). The pressure acting on the wall facing was smaller than the pressure to be resisted by the nails and averaged $0.32K_a\gamma H_t$.

The locus of the position of the maximum force T_{max} in that nail followed a classical parabolic shape going through the bottom of the wall and intersecting the top of the

wall at $0.7H_e$ or the bridge deck level at $0.5H_t$ (Fig. 8).

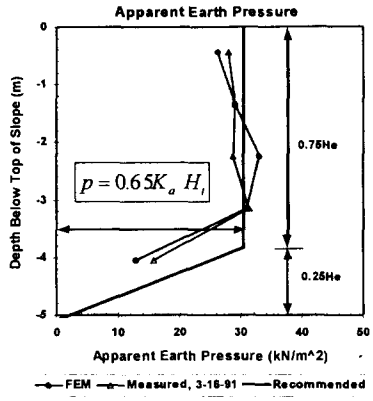

Fig.7. Earth Pressure Diagrams from Maximum Nail Forces

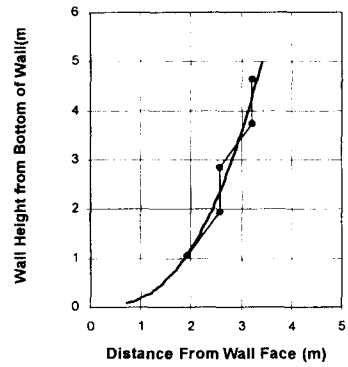

Fig.8. Predicted Locus of Maximum Nail Force

If was found that 60-70% of T_{max} in a nail was generated by the excavation step following the installation of that nail and that 90% of T_{max} was reached after two excavation steps. The maximum force T_{max} that will exist in a nail can be estimated from the apparent pressure that the wall has to resist. This pressure appears to be well estimated for all nails except the bottom one by

$$p = 0.65\ K_a \gamma H_t \tag{5}$$

The pressure for the bottom nail is $1/2p$. The maximum force T_{max} in all nails except the bottom one is given by

$$T_{max} = 0.65\ K_a \gamma H_t b\ S_v \tag{6}$$

where b=nail horizontal spacing (equal to the pile spacing); and S_v=vertical nail spacing.

7.2 Downdrag Load on Piles

The excavation of the slope leads to a significant downdrag load on the piles. The maximum downdrag load was 260kN per pile and occured at the bottom of the excavation (Fig. 9, 10). The downdrag load accumulates from the level of the bridge deck down to the bottom of the excavation where it reaches a maximum value F_{Dmax}. The value of F_{Dmax} can be estimated by

$$F_{Dmax} = 0.65\ K_a \gamma b H_t^2 \tan\phi \tag{7}$$

where b=pile spacing and Φ=soil friction angle. This equation assumes that one pile carries the downdrag created over the entire triabutary area of that pile (b wide, H_t high), that the pressure on that area is $0.65K_a\gamma H_t$, and that the downdrag is the

horizontal load multiplied by the coefficient of friction (tan Φ)

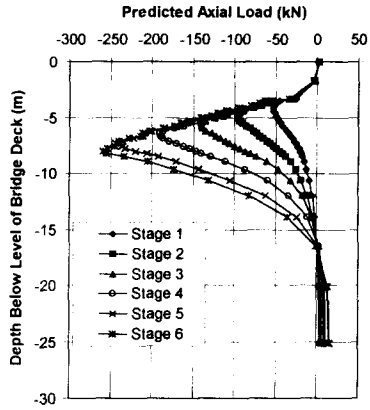

Fig.9. Axial Loads Induced in Pile by Excavation Steps

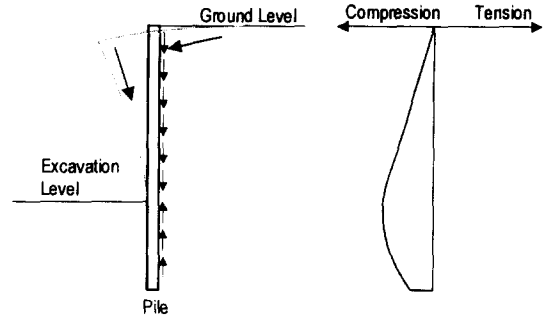

Fig.10. Axial Load due to Downdrag of Soil Mass

7.3 Bending Moments in Piles

The excavation of the slope also leads to an additional bending moment in the piles. The maximum bending moment was 22kN-m per pile and occured near the bottom of the excavation (Fig.11). The moment is caused by the soil pressure behind the piles and reaches a maximum value M_{max} is slightly above the excavation level. The maximum moment can be estimated by

$$M_{max} = \frac{K_a \gamma b H_t^3}{200} \tag{8}$$

This equation assumes that the horizontal distributed load on the pile is constant and equal to $0.65K_a\gamma H_t$, that M_{max} acts at the bottom of the excavation where the moment arm is $H_t/2$ (Fig.12).

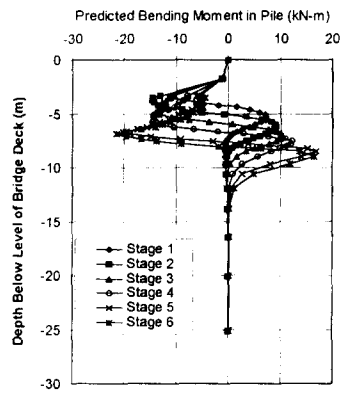

Fig. 11. Bending Moment Induced in Pile by Excavation Steps

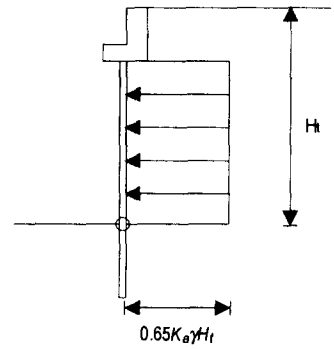

Fig.12. Calculation of Maximum Bending Moment

Both the downdrag load and the bending moment represent additional values solely due to the excavation of the slope because the piles were modeled as stress free before the FEM simulation of the excavation of the slope began.

7. Conclusions

The following conclusions and recommendations are drawn:

1. This study pertains to soil nailed walls under piled bridge abutment. The soil nailing technique can be applied to the road expansion successfully by removing the slope embankment under the bridge in front of the abutment
2. The maximum nail force can be estimated from the apparent earth pressure that the wall has to resist. The locus of the position of the maximum force in the nail follows a classical parabolic shape.
3. Excavation of the slope induces significant downdrag load on the piles. The maximum downdrag load occurred at the bottom of the excavation.
4. The excavation of the slope leads to an additional bending moment in the piles. The maximum bending moment occurred near the bottom of the excavation.
5. The maximum downdrag load and bending moment can be calculated by considering the apparent earth pressure.

References

1. ABAQUS User's and Theory Manuals. (1992). Version 5.2
2. CALTRANS. (1994). SNAIL Program and User's Manual, Version 2.05
3. Lim, Y.-J. (1996). Three-Dimensional Nonlinear Finite Element Analysis of Tieback walls and of Soil Nailed Walls Under Piled Bridge Abutments. *Ph.D. Dissertation*, Texas A&M University, College Station, Texas, U.S.A.
4. Lim, Y.-J., and Briaud, J. L. (1996). Three-Dimensional Nonlinear Finite Element Analysis of Tieback walls and of Soil Nailed Walls Under Piled Bridge Abutments. *Report to the Federal Highway Administration and the Texas Department of Transportation*, Department of Civil Engineering, Texas A&M University, College Station, Texas, U.S.A.
5. Seed, R. B. and Duncan, J. M.(1984). "SSCOMP: a finite element analysis program for evaluation of soil-structure interaction and compation effects." Report No. UCB/GT/84-02, University of California, Berkely.